



Model Predictive Control of a Medical Robotic System

Ivan Buzurovic^(✉)

Harvard Medical School, Harvard University, Boston, MA 02115, USA
ibuzurovic@bwh.harvard.edu

Abstract. One of the most challenging phases in interstitial brachytherapy is the placement of the needles. In these medical procedures, the needles are inserted inside the tissue to guide the positioning of the radioactive sources. The low dose-rate (LDR) radioactive sources are placed inside the tissue permanently, whereas a radioactive source in the high dose-rate (HDR) brachytherapy is temporarily placed in the desired positions so that the delivery of the prescription dose to the clinical targets can be achieved. Therefore, it is important to develop a robust and sophisticated tool that can perform the automatic needle placement with a high level of accuracy for different medical procedures and conditions. In this study, we propose a novel concept for the automatic needle insertion using a new miniature automated robotic system. The mathematical model of this system was derived, allowing the implementation of the model predictive control (MPC) that can be used to govern the mechanism. The purpose of this approach was to minimize the lateral components of the generalized reactive force which is responsible for the tissue displacement and, consequently, for the needle deflection.

Keywords: Robotic system · Model predictive control · Needle insertion

1 Introduction

In contemporary brachytherapy, the accurate positioning of the needles into the pre-defined locations is a challenging and complex task due to a variety of reasons [1]. The precision and reproducibility of the needle placement in manual brachytherapy procedures are highly dependent on the experience and dexterity of the physicians [2]. Some of the major problems that appear during the needle insertion in brachytherapy are caused by the displacement and deformation of the soft tissue. Prostate deformation as well as possible calcifications within the gland or denser tumour tissue can cause needle deflection and needle clustering, which is hard to track and estimate. The lack of spatial resolution in ultrasound imaging or lack of the real-time needle position estimation in interstitial brachytherapy makes the implementation of the automatic corrections especially difficult. Needle deflection and displacement can result in significant dosimetric discrepancies in the clinical practice if the position error was not assessed and encountered. For instance, if the needle placement accuracy was ± 1 mm, there

exists a dose variation between 58% and 274% for a 40.7 cGy cm²/h source of a high dose-rate (HDR) after loader at the point located 2 mm distal to the tip of the needle, as previously reported in [3].

Several researchers have analysed these problems. Thus, a variety of approaches were proposed to improve the insertion strategies [2, 4–11]. Some of the suggested methodologies included the evaluation of different trajectories (such as curvilinear or flexible insertions), correlation of the tissue deformation and the infinitesimal force per tissue displacement for the real-time updates of the needle trajectories, or different models capable of predicting the deformation of the tissue caused by needle insertions, etc. However, most these strategies have remained academic. Recently, several authors have reported the design, investigation and development of the image-guided robotic-based systems for the brachytherapy and biopsy procedures that included automatic needle insertions [3, 12–20]. The purpose of the listed systems was to accurately place the needles into the desired locations using robot assisted automatic or semi-automatic insertions. To the best of our knowledge, none of these robotic systems is in clinical use.

Considering the significance of the topic, we propose a novel approach to the automated needle insertion. Furthermore, we outlined the requirements for the development of a portable handheld ($n + 2$) degree-of-freedom (DOF) automatic device for needle insertion. This device can incorporate the proposed insertion strategies with the goal to insert the needle with a high level of accuracy. To achieve this goal, we report the detailed mathematical model for the proposed system. The main purpose of the mathematical model approach was twofold: (a) the mathematical model should accurately represent the relevant physical phenomena that significantly influence the system dynamics of such device, and (b) the mathematical model should be suitable for implementation in the real-time computations. Therefore, the presented mathematical model has a practical component rather than an academic value solely. In addition, the results were supported with extensive computer simulations. The proper choice of the control methodology is crucial to achieve the accurate needle placement under different scenarios such as the variety of tissue responses to the insertion force, different lateral components of the forces to the needle and, consequently, the needle deflection. Ideally, the control method should be able to correct the needle deflection during the insertion, or to prevent the deflection by minimizing the lateral insertion forces. In the proposed method, we apply the model predictive control (MPC) as a possible control method capable of achieving the desired dynamical behaviour of the system. The detailed implementation of the MPC prior to the simulation of the system was also presented in this article.

2 Mathematical Model of the System

To be able to perform the simulation of the system and to analyse the needle insertion parameters, the following steps were performed: (a) analysis of kinematics of the PIN, (b) development of the dynamic equations of motion for the PIN, and (c) development and simulation of a kinematic and dynamic control algorithm using the MPC.

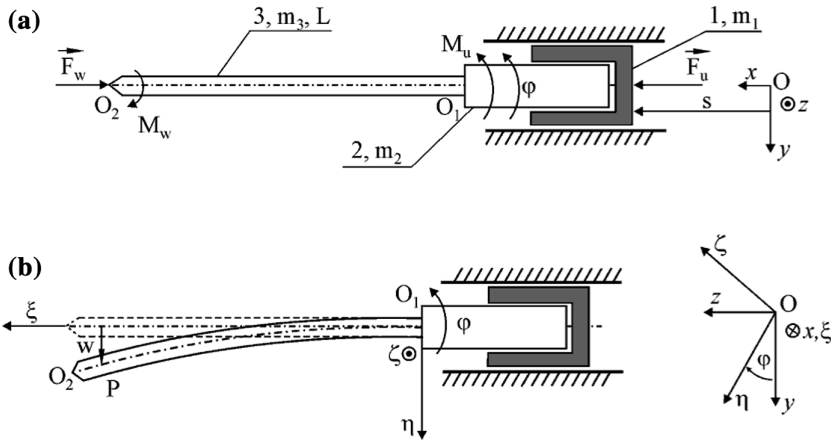


Fig. 1. (a) External schematic view of the mechanism with a needle (PIN), (b) The mechanism in the arbitrary moment during the needle insertion. The fixed and movable coordinate systems were presented.

Figure 1a represents the model of the proposed mechanism with a needle named PIN. It consists of the needle holder 1 having mass m_1 . The needle holder moves in the translational direction along the straight guidance rail. The model of the mechanism included a rotational part of the needle holder, marked as 2, having mass m_2 and axial inertia moment I_2 with respect to the rotational axes. The elastic needle 3 is the third part of the mechanism connected to the end O_1 , and it is represented as a cantilever beam. In Fig. 1a, s denotes the motion of the needle holder 1 along the guiding rail, and φ is the rotational angle of needle holder 2. The control force F_u acts upon the holder and control torque M_u acts upon the rotational joint 2. During the needle insertion procedures, the resistant torque M_w acts against the needle rotation as well as resistant force F_w that acts upon the needle tip O_2 , as shown in Fig. 1a. It is assumed that the force F_w is parallel to the axis x during the motion of the needle.

The needle itself is represented as an elastic beam with n DOF. With this purpose in mind, the analyzed mechanical system has indefinite degrees of freedom. Since the mechanism consists of rigid and elastic bodies, the system belongs to the group of hybrid systems. The dynamical behavior of such systems is represented with both differential equations and partial differential equations. To increase the real-time calculations without losing precision, the methodology called the assumed-modes method was used for the mathematical modeling [3]. In this approach, the dynamics of the elastic needle was analyzed using a finite number of degrees of freedom. The configuration of the mechanism at the arbitrary moment during the needle insertion was presented in Fig. 1b. The frame O_{xyz} is the inertial frame of reference with O_{xy} representing a vertical plane. The moving coordinate frame $O_1\xi\eta\zeta$ is fixed to body 2 in such manner that the axis ζ coincides with the needle axis in its non-deformed configuration. The differential equations of the motion of the system considered can be obtained by means of the Lagrange equation,

$$\frac{d}{dt} \left(\frac{\partial L}{\partial \dot{\mathbf{q}}_r} \right) - \frac{\partial L}{\partial \mathbf{q}_r} = \mathbf{Q}_r, \quad \frac{d}{dt} \left(\frac{\partial L}{\partial \dot{\mathbf{q}}_f} \right) - \frac{\partial L}{\partial \mathbf{q}_f} = \mathbf{Q}_f \quad (1)$$

where $L = T - V$ is the Lagrangian function. Equation (1) can be written in the following matrix form:

$$\begin{bmatrix} \mathbf{M}_{rr} & \mathbf{0}_{2 \times n} \\ \mathbf{0}_{n \times 2} & \mathbf{M}_{ff} \end{bmatrix} \begin{bmatrix} \ddot{\mathbf{q}}_r \\ \ddot{\mathbf{q}}_f \end{bmatrix} + \mathbf{h}(\dot{\mathbf{q}}_r, \dot{\mathbf{q}}_f, \mathbf{q}_f) + \begin{bmatrix} \mathbf{0}_{2 \times 2} & \mathbf{0}_{2 \times n} \\ \mathbf{0}_{n \times 2} & \mathbf{K} \end{bmatrix} \begin{bmatrix} \mathbf{q}_r \\ \mathbf{q}_f \end{bmatrix} = \begin{bmatrix} \mathbf{Q}_r \\ \mathbf{Q}_f \end{bmatrix} \quad (2)$$

where, $\mathbf{h}(\dot{\mathbf{q}}_r, \dot{\mathbf{q}}_f, \mathbf{q}_f) = [0, 2m_3 \left(\sum_{i=1}^n q_{if} \dot{q}_{if} \right) \dot{\phi}, -m_3 q_{1f} \dot{\phi}^2, -m_3 q_{2f} \dot{\phi}^2, \dots, -m_3 q_{nf} \dot{\phi}^2]^T R^{(2+n) \times 1}$.

This model represents the basis for the development of the needle insertion control that should minimize the lateral insertion force and needle deflection. The model does not incorporate the potential energy of the needle due to gravity force since it does not influence the overall system dynamics. Finally, the system (3) can be transformed to a non-linear state-space form as follows:

$$\begin{aligned} \dot{\mathbf{x}}(t) &= \mathbf{A}(t)\mathbf{x}(t) + \mathbf{B}(t)\mathbf{u}(t) + \mathbf{v}(t) \\ \mathbf{y}(t) &= \mathbf{C}(t)\mathbf{x}(t) + \mathbf{w}(t) \end{aligned}, \quad (3)$$

where $\mathbf{x}(t)$, $\mathbf{u}(t)$ and $\mathbf{y}(t)$ are state vector, control vector and output vector, respectively; $\mathbf{v}(t)$ and $\mathbf{w}(t)$ are state disturbance and measured disturbance vectors; $\mathbf{A}(t)$, $\mathbf{B}(t)$ and $\mathbf{C}(t)$ are corresponding time varying state matrix, input matrix and output matrix, respectively. Following the procedure reported in [20], the matrices $\mathbf{A}(t)$, $\mathbf{B}(t)$ and $\mathbf{C}(t)$ are calculated as: $\mathbf{A}(t) = [\mathbf{0} \ \mathbf{0} \ \mathbf{I} \ \mathbf{0}; \ \mathbf{0} \ \mathbf{0} \ \mathbf{0} \ \mathbf{I}; \ \mathbf{0} \ \mathbf{0} \ \mathbf{0} \ \mathbf{0}; \ \mathbf{0} \ \mathbf{K}/\mathbf{M}_{ff} \ \mathbf{0} \ \mathbf{0}]$, $\mathbf{B}(t) = [\mathbf{0} \ \mathbf{0} \ \mathbf{1}/\mathbf{M}_{rr} \ \mathbf{1}/\mathbf{M}_{ff}]^T$, and $\mathbf{C}(t)$ is equal to identity matrix since the generalized positions and velocities are chosen to be the system output. In addition, $\mathbf{x}(t) = [\mathbf{x}_1 \ \mathbf{x}_2 \ \mathbf{x}_3 \ \mathbf{x}_4]^T$, $\mathbf{x}_1 = \mathbf{q}_r$, $\mathbf{x}_2 = \mathbf{q}_f$, $\mathbf{x}_3 = \dot{\mathbf{q}}_r$, and $\mathbf{x}_4 = \dot{\mathbf{q}}_f$. Consequently, $\mathbf{v}(t) = [\mathbf{0} \ \mathbf{0} \ \mathbf{0} - \mathbf{h}_1(\mathbf{x}_2, \mathbf{x}_3, \mathbf{x}_4)]^T$, where $\mathbf{h}_1(\mathbf{x}_2, \mathbf{x}_3, \mathbf{x}_4)$ is the second element of the $\mathbf{h}(\dot{\mathbf{q}}_r, \dot{\mathbf{q}}_f, \mathbf{q}_f) = [0, h_1(\dot{\mathbf{q}}_r, \dot{\mathbf{q}}_f, \mathbf{q}_f)]$ transformed to its state space form.

3 Model Predictive Controller

The MPC operates by finding the adequate control solution in an iterative process, incorporating the system dynamics, measurements and disturbances into the calculations. The schematic representation of the process is presented in Fig. 2. In this specific case, the formulation of the control procedure is as follows: based on the measurements of the resistance force F_w that acts upon the needle tip, the controller predicts the system behavior over the prediction horizon T_p , and calculates the input (F_u and M_u) of the system over the control horizon T_c . This calculation is performed such that the performance objective is minimized. In this case, the lateral displacement of the needle \mathbf{R}_w is minimized.

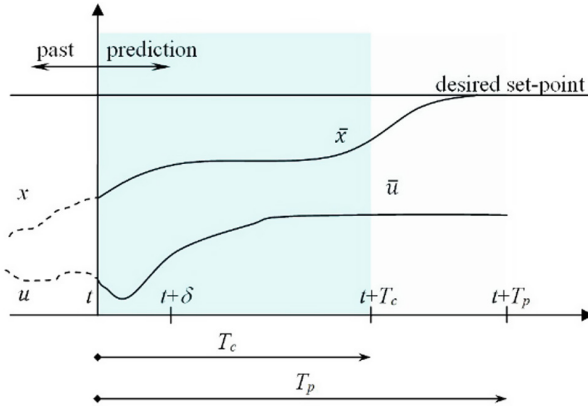


Fig. 2. General representation of the MPC functionality.

Consequently, the basic task of the MPC is to calculate the insertion speed represented by the motor driving force F_u , and the rotational speed of the needle represented by the motor driving torque M_u so that the lateral displacements of the needle tip and the lateral components of the insertion force over the sampling period can be minimized. This calculation is performed iteratively in real-time to allow for the needle steering with variable translational and rotational speeds. In the case when the lateral force components and the lateral displacement are zero, the controller continues to operate, using the same parameters until the desired behavior is maintained. The sampling time δ can vary to save the calculation time, but it is usually set to be fixed. The calculated system states at the instant $t + \delta$ let both the control procedure and the prediction horizon move forward. For this case, the linear model of the system would be insufficient to describe the process adequately; therefore, a nonlinear model was used for a more accurate representation of the process.

The overall purpose of the control task is to change the control parameters, such as the rotational and translational speed, and to obtain the rectilinear insertion makes the reference constant. In this work, we analyze a more conservative case – rectilinear needle insertion; however, this reference does not need to be constant and the system is potentially capable of needle steering in the 3D space. In general, to allow for the optimal needle placement inside the tissue for the brachytherapy procedures, we propose to minimize the lateral components of the insertion force (resistance force), and to predict and compensate for the influence of both the measured and unmeasured disturbances before their effect influences the system behavior i.e. needle displacement from the desired position. With this control strategy, it is possible to minimize both forces during the insertion and lateral displacement and, consequently, the needle deflection. The system receives information about the measured reactive force and tunes the parameters such as the translational speed and needle rotation in real-time during the insertion.

Referring to Fig. 3, the following parameters and variables are represented in the block diagram: D_{unm} represents the unmeasured disturbances to the system. These disturbances, such as the tissue resistance or lateral forces, increase the needle deflection during the procedure. The deflection depends on the insertion force, and based on that

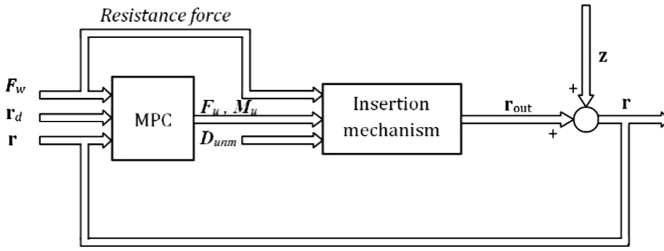


Fig. 3. Block diagram of the MPC for the needle insertion procedure using a proposed mechanism.

value, it can be estimated with a satisfactory level of accuracy, as in [1]. \mathbf{r}_d is the vector that represents all reference position values, i.e. the desired needle tip position, during the insertion. This value is the targeting value of the output. The task of the system is to decrease the lateral components of the actual insertion force to minimize the deflection and, consequently, to meet the criteria for this setpoint. The resistance force F_w is a measured disturbance of the system for which the MPC provides a feedforward compensation to decrease its influence on the needle position. F_u and M_u are the generalized torques of the motors, as previously described. These control signals are adjusted in real-time to achieve the objectives of the system. The output of the systems is denoted as \mathbf{r}_{out} , and it is a real needle tip position during the insertion. This value is a controlled variable of the system. \mathbf{r} is the output of the system, i.e. the calculated tip position that was used for the estimation of \mathbf{r}_{out} . The signal \mathbf{z} represents the disturbance vector that contains the unpredicted influences on the system. The disturbance vector includes the electrical and actuator noises, calibration uncertainties, and inaccuracies due to the modeling of the physical system as well as other unpredicted effects on the system. The described approach is challenging and highly dependent on the accuracy of the mathematical model of the process. That is the basic reason why the equation of the motion (2) is crucial for further development. The second challenge in this approach is the proper individual tuning of the parameters, such as the adjustments of the actuators and the selection of the proper weights to allow for a minimal deviation of the desired deflection over its set-points within the prediction horizon.

In the situation when complicated physical processes related to needle tissue interaction are analyzed, two opposite requirements arise: the possibility of the development of an accurate mathematical model and, on the other hand, the possibility to implement the proposed method to the real-time procedure with highly demanded data processing and computation. The insertion procedure should be performed only in few seconds. The most suitable controller for such tasks should can minimize the influence of the unknown system disturbances and deviations in mathematical modeling, while obtaining the measurements from the environment for the corrected control output. Therefore, it was decided to use a model predictive controller (MPCN). The MPCN is the key component of the proposed system. The proposed controller can predict and compensating for the unmeasured disturbances, such as the needle deflection or tissue reactive force, and it can correct them without waiting until the effect appears at the output of the system. On the other hand, the controller can

maintain the desired needle tip position within the predefined limits, allowing for a high level of accuracy. Since the system model (3) is the system of a differential non-linear equation, the MPCN is also non-linear. It means that this approach required the iterative solution of an optimal control problem.

In this part, the basic functionality of the MPC is described. Initially, the MPC controller solves the linear-quadratic-Gaussian optimization problem for our multi-input multi-output system. For the system (25), the following cost function has been minimized,

$$J = E \left(\mathbf{x}^T(T)F\mathbf{x}(T) + \int_0^T (\mathbf{x}^T(t)Q(t)\mathbf{x}(t) + \mathbf{u}^T(t)R(t)\mathbf{u}(t))dt \right) \quad (4)$$

where E denotes the vector of the reference values or setpoints; T is the time horizon that can be finite or equal to $+\infty$, depending on the time during which it is necessary to perform the insertion of the individual needle. When $T \rightarrow +\infty$, $\mathbf{x}^T(T)F\mathbf{x}(T) \rightarrow 0$. The goal of the optimization process is to find the feedback gain matrix $L(t)$ i.e. the proper torques for the motors that will guarantee the desired dynamic behavior of the system. Consequently,

$$L(t) = R^{-1}(t)B^T(t)S(t) \quad (5)$$

where $S(t)$ is the solution of the following Ricatti differential equation:

$$\dot{S}(t) = -A^T(t)S(t) - S(t)A(t) + S(t)B(t)R^{-1}(t)B^T(t)S(t) - Q(t) \quad (6)$$

The control algorithm with multiple variables uses the optimization function (30) together with the internal dynamics (25) of the system. For the control process, the information about the past controlled motions was used to calculate the optimal dynamical behavior during insertion.

$$J = \sum_{i=1}^N w_{x_i} (r_i - x_i)^2 + \sum_{i=1}^N w_{u_i} \Delta u_i^2 \quad (7)$$

where x_i is the needle tip position, r_i is the reference needle tip position, u_i is the control signal from the actuators, w_{x_i} is the weighting coefficient responsible for the relative importance of the x_i , whereas w_{u_i} is the weighting coefficient that penalizes the large change in gradient of u_i . Thus, the optimization cost function with the proper choice of the coefficients (7) ensures the decay of the transient errors as well as the reduction of the steady-state errors.

4 Results

The insertion accuracy was evaluated when the MPCN governed the needle insertion system represented by the Eq. (3). A representative case of the needle tip trajectory was presented in Fig. 4. Under the influence of the measured force, it was revealed that it

was possible to minimize the needle deflection and to insert the needle into the desired position with the highest level of accuracy when the MPC approach was used. Additionally, Fig. 4 shows the simulation results when the $M_u = 0$ *i.e.* when the actuator dedicated to the needle rotation was turned off.

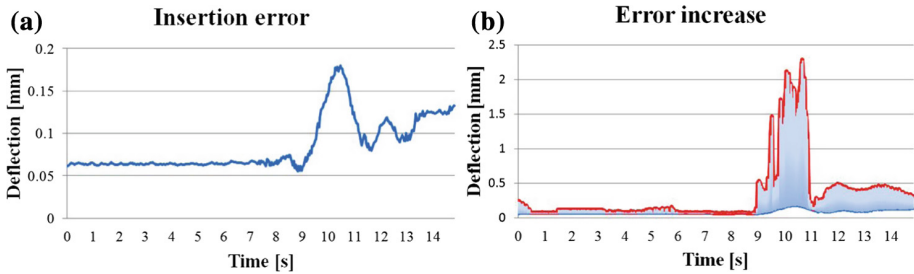


Fig. 4. Needle deflection (a) with and (b) without rotation control component (a representative case). An increase in the error was noticed when the needle rotation was not included into the process (marked region).

The simulation was performed under the influence of the recorded forces during the experiments. This conclusion proved the concept that the control of the translational motion was not sufficient and could not minimize the deflection up to the level at which the needles would not deflect significantly. Consequently, in this simulation, we proved the importance of the needle rotation for the accurate needle placement. When the simulation was repeated for different insertion depths (from 4 cm to 10 cm), it was revealed that the average needle tip displacements in the x , y and z directions were, -0.09 mm, 0.19 mm and 0.12 mm with an average SD = 0.13 mm, respectively. The auto-correction of the needle heading angle was presented in Fig. 5. It was observed that the angle increased initially before the MPCN started to correct the lateral displacement and, consequently, to minimize the angle.

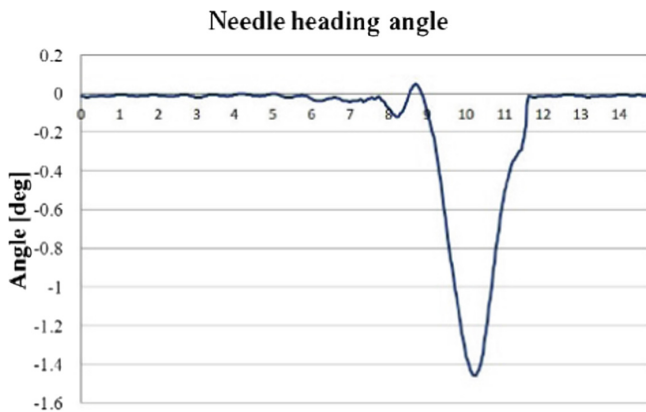


Fig. 5. Heading angle during insertion; MPCN corrects for the possible increase of the angle.

At this point, when the needle tip displacement is known, it is possible to use Eqs. (1) and (3) to recalculate the insertion forces. The values of the actuator parameters that lead to the insertions with minimal deflections are known as well. With the forward kinematics calculations of the system model, it is possible to calculate and re-evaluate the insertion forces achieved in the simulations. For this purpose, we recalculated the forces and the torques to evaluate if this process would result in any change of the measured insertion parameters. The results are presented in Fig. 6.

It was noticed that the torque on the insertion axis (z) did not change significantly whereas the x and y torques were minimized. This result was to be expected only if the lateral displacement of the needle was minimized. The torque on the insertion axis was not changed since it was necessary to apply the torque to allow for the needle insertion and steering. The similar observation was noticed in the case of the insertion force recorded at variable points of the needle during the procedures.

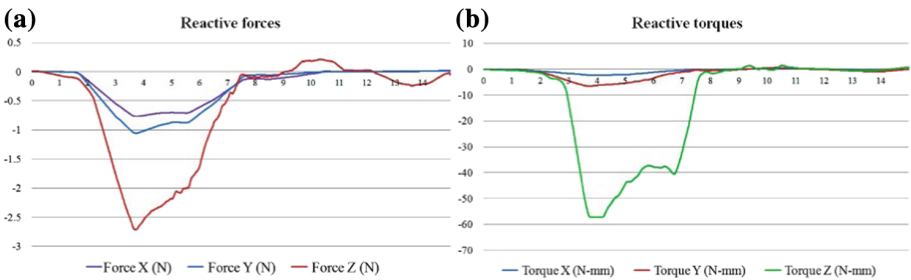


Fig. 6. Recalculated needle insertion parameters: (a) reactive forces in x , y and z directions, and (b) reactive torques on x , y and z axis (a representative case).

We compared the needle tip position accuracy to the accuracy achieved by the commonly used control strategies to evaluate the insertion accuracy when the MPC control approach and MPCN were used. The insertion system (Fig. 1) described by a mathematical model (2) was simulated using both the MPCN and the PID to evaluate the increase in accuracy when the MPC was used. The results were presented in Fig. 7.

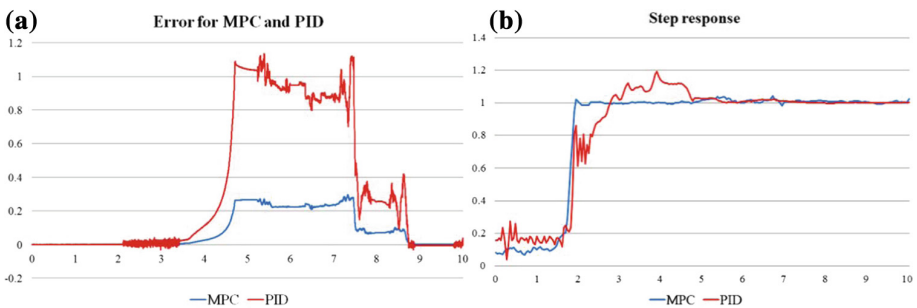


Fig. 7. Position error and (b) step response for MPC and PID needle control (a representative case).

It was noticed that the needle positioning accuracy was higher with the MPC method due to the needle steering provision, i.e. the adaptive change of the control parameters such as the velocity and rotational speed of the needle. When the response of both systems to the step function was evaluated, it was noticed that the transient parameters such as overshoot and settling time were more favorable in the MPC case. Whereas it is known that the PID ensures the asymptotic decay of the transient errors as well as reduction of the steady-state errors, the MPCN can deal with the overall system error without waiting until the effect appears at the output of the system regardless of whether the error is caused by the different modeling approaches or other unknown influences on the analyzed system. The overall conclusion was that the MPC approach was a preferred control methodology for the automatic needle insertion due to the described advantages over the PID control.

5 Conclusion

In this article, we presented a novel approach to the needle insertion. The controlled needle insertion using a predictive controller required a high level mathematical model of the physical process. Due to that fact, the mathematical model of the robotic system with $(n + 2)$ DOF was presented. The needle was an elastic beam modelled with n DOF using the assumed-mode method. Using the adequate control methodology (MPC), it was possible to minimize the reactive force that was directly responsible for the needle deflection and needle tip displacement. Consequently, it was possible to guide the needle in a way which allowed for the maximum accuracy and minimal needle deflection. The future work will include the manufacturing of a mobile, portable and programmable robotic needle insertion mechanism with potential to be implemented in various medical procedures where the needle insertion must be performed with high reliability and accuracy, such as in interstitial brachytherapy, biopsy and other relevant procedures. The comparison between other control methodologies (such PID or adaptive control) and the MPC can potentially lead to clinically relevant results. The non-rectilinear needle insertion including the variable reference can be additionally investigated. In addition, the clinical trials using the proposed device are part of the future work so that the limitations and the possible advantages of this device should be adequately addressed in various clinical settings.

References

1. Buzurovic, I., Podder, T.K., Yu, Y.: Prediction control for brachytherapy robotic system. *J. Robot.* **1**, 1–10 (2010)
2. Buzurovic, I., et al.: Real-time control strategy for collision avoidance and seed deposition in brachytherapy robotic system. *Int. J. Comput. Assist. Radiol. Surg.* **3**, 30–34 (2008)
3. Siebert, F.A., Hirt, M., Niehoff, P., Kovács, P.: Imaging of implant needles for real-time HDR-brachytherapy prostate treatment using biplane ultrasound transducers. *Med. Phys.* **36** (8), 3406–3412 (2004)

4. Abolhassani, N., Patel, R., Moallem, M.: Trajectory generation for robotic needle insertion in soft tissue. In: Proceedings of the 26th IEEE International Conference on Engineering in Medicine and Biology (EMBS), San Francisco CA, USA, pp. 2730–2733 (2004)
5. Alterovitz, R., Goldberg, K., Pouliot, J., Taschereau, R., Hsu, I.-C.: Sensorless planning for medical needle insertion procedures. In: Proceedings of the IEEE/RSJ International Conference on Intelligent Robots and Systems, Las Vegas, NV, USA, pp. 3337–3343 (2003)
6. Chui, C.-K., Teoh, S.-H., Ong, C.-J., Anderson, J.H., Sakuma, I.: Integrative modeling of liver organ for simulation of flexible needle insertion. In: Proceedings of the 9th IEEE International Conference on Control, Automation, Robotics and Vision (ICARCV), Singapore, pp. 1–6 (2006)
7. Crouch, J.R., Schneider, C.M., Wainer, J., Okamura, A.M.: Velocity-dependent model for needle insertion in soft tissue. In: Proceedings of the 2005 Medical Image Computing and Computer-Assisted Intervention (MICCAI 2005), pp. 624–632 (2005)
8. DiMaio, S.P., Salcudean, S.E.: Needle insertion modeling and simulation. *IEEE Trans. Robot. Autom.* **19**(5), 864–875 (2003)
9. DiMaio, S.P., Salcudean, S.E.: Interactive simulation of needle insertion models. *IEEE Trans. Biomed. Eng.* **52**(7), 1167–1179 (2005)
10. Okamura, A.M., Simone, C., O’Leary, M.D.: Force modeling for needle insertion into soft tissue. *IEEE Trans. Biomed. Eng.* **51**(10), 1707–1716 (2004)
11. Wan, G., Wei, Z., Gardi, L., Downey, D.B., Downey, D.B., Fenster, A.: Brachytherapy needle deflection evaluation and correction. *Med. Phys.* **32**(4), 902–909 (2005)
12. Buzurovic, I., Tarun, K., Yu, Y.: Robotic systems for radiation therapy. In: Dutta, A. (ed.) *Robotic Systems: Applications, Control and Programming*, pp. 85–106. InTech, Rijeka (2012)
13. Fichtinger, G., Burdette, E.C., Tanacs, A., Patriciu, A., Mazilu, D., Whitcomb, L.L., et al.: Robotically assisted prostate brachytherapy with transrectal ultrasound guidance: phantom experiments. *Brachytherapy* **5**, 14–26 (2006)
14. Lin, A., Trejos, A.L., Patel, R.V., Malthaner, R.A.: Robot-assisted minimally invasive brachytherapy for lung cancer. *Telesurgery* **4**, 35–52 (2008)
15. Meltsner, M.A., Ferrier, N.J., Thomadsen, B.R.: Observations on rotating needle insertions using a brachytherapy robot. *Phys. Med. Biol.* **52**, 6027–6037 (2007)
16. Moerland, M.A., Van den Bosch, M.R., Lagerburg, V., Battermann, J.J., Van Vulpen, M., Lagendijk, J.J.W.: An MRI scanner compatible implant robot for prostate brachytherapy. *Brachytherapy* **7**(2), 100 (2008)
17. Wei, Z., Wan, G., Gardi, L., Mills, G., Downey, D., Fenster, A.: Robot-assisted 3D-TRUS guided prostate brachytherapy: system integration and validation. *Med. Phys.* **31**, 539–548 (2004)
18. Buzurovic, I., Podder, T.K., Yan, K., Hu, Y., Valicenti, R., Dicker, A., Yu, Y.: Parameter optimization for brachytherapy robotic needle insertion and seed deposition. *Med. Phys.* **35** (6), 2865 (2008)
19. Buzurovic, I., Podder, T.K., Yu, Y.: Force prediction and tracking for image-guided robotic system using neural network approach. In: Proceedings of the IEEE Biomedical Circuits and Systems Conference (BioCAS), Baltimore MA, USA, pp. 41–44 (2008)
20. Buzurovic, I., Debeljkovic, D.: A Geometric approach to the investigation of the dynamics of constrained robotic systems. In: Proceedings of the IEEE International Symposium on Intelligent Systems and Informatics (YSI), Subotica, Serbia, pp. 133–138 (2010)